

# Initialization Method for Factorization Machine Based on Low-Rank Approximation for Constructing a Corrected Approximate Ising Model

Yuya Seki<sup>1</sup>, Hyakka Nakada<sup>1,2</sup>, and Shu Tanaka<sup>1,3,4,5</sup>

<sup>1</sup>Graduate School of Science and Technology, Keio University,  
Kanagawa 223-8522, Japan

<sup>2</sup>Recruit Co., Ltd., Tokyo 100-6640, Japan

<sup>3</sup>Department of Applied Physics and Physico-Informatics, Keio  
University, Kanagawa 223-8522, Japan

<sup>4</sup>Keio University Sustainable Quantum Artificial Intelligence Center  
(KSQAIC), Keio University, Tokyo 108-8345, Japan

<sup>5</sup>Human Biology-Microbiome-Quantum Research Center  
(WPI-Bio2Q), Keio University, Tokyo 108-8345, Japan

This paper presents an initialization method that can approximate a given approximate Ising model with a high degree of accuracy using the Factorization Machine (FM), a machine learning model. The construction of Ising models using FM is applied to the combinatorial optimization problem using the factorization machine with quantum annealing. It is anticipated that the optimization performance of FMQA will be enhanced through the implementation of the warm-start method. Nevertheless, the optimal initialization method for leveraging the warm-start approach in FMQA remains undetermined. Consequently, the present study compares a number of initialization methods and identifies the most appropriate for use with a warm-start in FMQA through numerical experimentation. Furthermore, the properties of the proposed FM initialization method are analyzed using random matrix theory, demonstrating that the approximation accuracy of the proposed

method is not significantly influenced by the specific Ising model under consideration. The findings of this study will facilitate the advancement of combinatorial optimization problem-solving through the use of Ising machines.

## 1 Introduction

Factorization machine with quantum annealing (FMQA) [1] is a black-box combinatorial optimization method that combines annealing technology and machine learning. Annealing is a metaheuristic for combinatorial optimization problems. Two distinct types of annealing are recognized: quantum annealing (QA) [2–4], which exploits quantum effects, and simulated annealing (SA) [5–7], which utilizes temperature effects. The development of annealing devices that implement these optimization methods has enabled the rapid solution of combinatorial optimization problems [8–19]. For example, a device that performs quantum annealing has been developed, and a system comprising over 5,000 superconducting qubits is currently available for use [20]. Moreover, the development of annealing devices that do not utilize quantum effects is also currently underway. To use these annealing devices, it is often necessary to express the objective function of the combinatorial optimization problem as a quadratic unconstrained binary optimization (QUBO) or as a Hamiltonian of an Ising model that is equivalent to QUBO. It is well-established that the objective function of numerous combinatorial optimization problems can be expressed as an Ising model [21].

Nevertheless, there are instances where the objective function of a combinatorial optimization problem cannot be expressed in an exact form using the Ising model. In particular, it is not feasible to derive an Ising model representation of the objective function for black-box combinatorial optimization problems. This is due to the fact that, in the case of black-box combinatorial optimization problems, the analytical form of the objective function, referred to as the “black-box function,” is not provided, and thus it is not feasible to formulate the objective function using an Ising model. FMQA is a model-based optimization method that has been developed to address this issue. In FMQA, an Ising model that approximates the black-box function is constructed based on the analysis of several input-output relationships associated with the black-box function. Subsequently, the Ising machine is employed to identify the optimal solution of the constructed Ising model. The machine learning model employed for the construction of the Ising model is the Factorization Machine (FM), as described in Ref. [22]. The training dataset for the FM is constructed from samples explored by the Ising machine. By alternating between sampling with the Ising machine and training the FM, the optimal solution is sought while simultaneously generating the samples necessary for training. As the model must be trained each time, the time required for this process can become a limiting factor of FMQA. Consequently, FMQA attains high-speed calculations through the utilization of FM, which possesses a minimal number of model parameters. Moreover, FMQA necessitates the estimation of an Ising model from a limited number of samples. According to Ref. [22], since FM accounts for the correlation between the components of training data points, it is possible to estimate a highly accurate model even

from a small number of samples. As can be observed, there are numerous advantages associated with the utilization of FM for the estimation of Ising models. The advent of FMQA has enabled the usage of Ising-machine-based high-speed solution searches for problems that were previously deemed inapplicable to Ising machines. This has led to a plethora of application studies [1, 23–32].

A novel application of FMQA is the enhancement of the precision of the approximate Ising model. Examples of applied research on Ising machines that derive an approximate Ising model and perform solution searches can be found in [33, 34]. The issue with this application is that if the approximation of the Ising model is of insufficient accuracy, it becomes challenging to search for low-energy solutions. One potential solution to this issue is to employ FMQA in the following manner. The initial step is to express the Hamiltonian of the Ising model, which is given as an approximation, in the form of FM. Subsequently, the FM model is employed as the initial model, and FMQA iterations are conducted. It is anticipated that an Ising model that rectifies the approximations inherent in the original model can be constructed using FM. By employing this refined Ising model in solution searches, it is expected that lower-energy solutions can be identified. This approach can be classified as a warm-start method in machine learning and mathematical optimization. In other words, by initiating the process with an FM model that is in close proximity to the true Ising model, it is possible to construct an Ising model with high approximation performance.

To apply the warm-start method to FMQA, it is necessary to develop an initialization method capable of reproducing the approximate Ising model using FM. The initialization method must utilize solely the information provided in the given approximate Ising model. Moreover, during the initial phase of FMQA, it is imperative that the FM model aligns with the initial Ising model. Otherwise, even if an FM model that is similar to the approximate Ising model is generated by initialization, the FM model will undergo changes that are not intended as a result of subsequent training. Accordingly, in order to construct a correction model for the approximate Ising model using FM, it is necessary for the distance between the FM model and the approximate Ising model to become closer when the FM is trained using the approximate Ising model dataset. In this paper, we perform a numerical analysis to determine an initialization method for FM that satisfies the aforementioned conditions. Additionally, we apply an analysis using random matrix theory, assuming that the interaction matrix of the approximate Ising model is generated according to a specific probability distribution. The analysis using random matrix theory demonstrates that the proposed initialization method exhibits minimal dependence on the specific instance of the target approximate Ising model.

The following is a description of the structure of this paper. In Sec. 2, we introduce the FM, which is the machine learning model utilized in this study. Subsequently, Sec. 3 delineates the initialization methodologies employed in the present study. In this section, we present two initialization methods for the FM model parameters. The first method is based on low-rank approximation of the interaction matrix of an approximate Ising model. The second method is a random initialization method that generates the FM model parameters from a probability distribution. In Sec. 4, we introduce an analysis method based on random matrix theory. In Sec. 5, we present the results of numerical

experiments and analysis based on random matrix theory to determine the initialization method for the FM with the desired properties. Finally, in Sec. 6, we provide a summary of the findings.

## 2 Factorization Machine

Factorization machines (FMs) constitute a specific type of machine learning model that can be utilized for regression, classification, and ranking problems [22]. The FM model is applied to a real vector of dimension  $N$ , represented as a column vector, namely,  $\mathbf{x} = (x_1, \dots, x_N) \in \mathbb{R}^N$ , and uses the following model equation, which returns a real number:

$$f_+(\mathbf{x}; \boldsymbol{\theta}) = w_0 + \sum_{i=1}^N w_i x_i + \sum_{\substack{i,j=1 \\ (i < j)}}^N \langle \mathbf{v}_i, \mathbf{v}_j \rangle x_i x_j, \quad (1)$$

where  $w_0 \in \mathbb{R}$ ,  $w_i \in \mathbb{R}$ ,  $\mathbf{v}_i \in \mathbb{R}^K$  are the model parameters of the FM determined by learning, and these are collectively represented as  $\boldsymbol{\theta}$ . Here, the natural number  $K$  is a hyperparameter of the FM. The sum of the quadratic terms is taken for all pairs of integers  $i$  and  $j$  that satisfy  $i < j$ , where  $i$  and  $j$  are two integers that take values from 1 to  $N$ . In addition, the interaction coefficient of the quadratic term,  $\langle \mathbf{v}_i, \mathbf{v}_j \rangle$ , represented by the inner product of the two vectors. In this paper, we designate the matrix with  $(i, j)$  component of  $\langle \mathbf{v}_i, \mathbf{v}_j \rangle$  as the interaction matrix of FM. In this case, the hyperparameter  $K$  represents the upper bound for the rank of the FM interaction matrix. For the sake of simplicity, henceforth, we will express the hyperparameter  $K$  as the rank of the FM. As stated in Ref. [22], the incorporation of the correlation between the components of the input variables into the model is made possible by the presentation of the interaction coefficients as inner products. This property enables the estimation of a highly accurate model even with a limited amount of training data. Another advantage of expressing interaction coefficients as inner products is that it reduces the amount of computation required. Although FM includes quadratic terms for the input variables, it is established that the time complexity for forward calculations is  $O(KN)$ . Moreover, the time complexity for calculating the partial derivatives necessary for estimating the model parameters during training is also  $O(KN)$ . As the computational time increases linearly with the input dimension  $N$ , the issue of FM learning becoming a bottleneck in FMQA, where the model must be trained repeatedly, can be circumvented. However, there is a limitation to the representational ability of FM, which is constrained by the fact that the interaction coefficients are expressed as inner products. It is not feasible to express arbitrary interaction coefficients in the form of inner products unless a sufficiently large  $K$  is employed (see below for details). Consequently, even if the model that generated the training data set is a quadratic function of the input variables, it is generally not possible to completely express that training data using FM.

The data set that can be expressed by FM is contingent upon the sign in the model equation. This property is referred to as the asymmetry of FM [35]. As a consequence

of this asymmetry, the behavior of the positive FM, as given by Eq. (1), the negative FM, as given below, are distinct:

$$f_{-}(\mathbf{x}; \boldsymbol{\theta}) = -w_0 - \sum_{i=1}^N w_i x_i - \sum_{\substack{i,j=1 \\ (i<j)}}^N \langle \mathbf{v}_i, \mathbf{v}_j \rangle x_i x_j.$$

Indeed, it has been demonstrated that the learning performance differs between positive FM and negative FM [36]. In this study, we conduct numerical experiments on both positive FM and negative FM, with the objective of selecting the model that exhibits superior learning performance.

This paper addresses the regression problem through the use of FM with input components that assume a value of either +1 or -1. In the regression problem, the objective is to identify the model parameters of the FM,  $\boldsymbol{\theta}$ , so as to minimize the loss function for the given dataset,  $\mathcal{D} = \{(\mathbf{x}_d, y_d) \in \{+1, -1\}^N \times \mathbb{R} \mid d = 1, \dots, D\}$ . In this paper, the mean-squared error, as defined below, is employed as the loss function:

$$L(\boldsymbol{\theta}) = \frac{1}{D} \sum_{d=1}^D (f(\mathbf{x}_d; \boldsymbol{\theta}) - y_d)^2, \quad (2)$$

where the function  $f$  is either  $f_{+}$  or  $f_{-}$ . In FM training,  $\boldsymbol{\theta}$  are updated repeatedly in the direction that minimizes the expression represented by Eq. (2). The number of updates required until the loss function converges depends on the initial value of the model parameters. Therefore, to reduce the calculation time required for training, an appropriate FM initialization method is necessary.

### 3 Initialization Methods for Factorization Machine

In this section, we introduce the method for initializing the model parameters of the FM. In this study, we assume that the Hamiltonian of the Ising model that approximates the model that generated the training data is available. The Hamiltonian is represented by

$$\begin{aligned} H(\mathbf{x}) &= c - \sum_{i=1}^N h_i x_i - \frac{1}{2} \sum_{\substack{i,j=1 \\ (i \neq j)}}^N J_{ij} x_i x_j \\ &= c - \sum_{i=1}^N h_i x_i - \sum_{\substack{i,j=1 \\ (i < j)}}^N J_{ij} x_i x_j, \end{aligned} \quad (3)$$

where  $c \in \mathbb{R}$  is a constant,  $h_i \in \mathbb{R}$  is a local magnetic field coefficient, and  $J_{ij} \in \mathbb{R}$  is an interaction coefficient. Here, the interaction coefficient is symmetric with respect to the subscript:  $J_{ij} = J_{ji}$ . In addition, the input variable takes a binary value of +1 or -1:  $\mathbf{x} = (x_1, \dots, x_N) \in \{+1, -1\}^N$ . For example, it is established that the cost function to be minimized in the problem of minimizing the energy of molecular adsorption on

a catalyst surface [34] and the problem of model compression in machine learning [33] can be approximated by an Ising model. In order to utilize FM for the enhancement of the precision of these specified approximate Ising models, it is essential to employ an initialization methodology that generates an FM model that is in close proximity to the approximate Ising model. The following sections introduce two FM model initialization methods. The first is a method that generates an initial FM model using the eigenvalue decomposition of the interaction coefficient matrix  $J = (J_{ij})$  of the given approximate Ising model. The second method generates an initial FM model that is close to the given approximate Ising model by adjusting the probability distribution that the model parameters follow.

### 3.1 Initialization by Eigenvalue Decomposition of Coupling Matrix

To generate an FM model that is close to an approximate Ising model, we only need to consider how to initialize the interaction coefficients. This is because the constant and linear terms of the FM model can be determined so that they match those of the given approximate Ising model:

$$\begin{cases} w_0 = +c, \\ w_i = -h_i \ (i = 1, \dots, N) \end{cases} \quad \text{for positive FM,}$$

$$\begin{cases} w_0 = -c, \\ w_i = +h_i \ (i = 1, \dots, N) \end{cases} \quad \text{for negative FM.}$$

Accordingly, we propose a methodology for approximating the interaction term of FM to the interaction term of the approximate Ising model:

$$\langle \mathbf{v}_i, \mathbf{v}_j \rangle \approx \begin{cases} -J_{ij} & \text{for positive FM,} \\ +J_{ij} & \text{for negative FM.} \end{cases}$$

In the following, we will limit our consideration to negative FM. The method for approximating positive FM is obtained by reversing the sign of the interaction coefficient  $J_{ij}$ .

The parameters of the FM interaction terms can be determined by low-rank approximation of the interaction matrix, denoted by  $J = (J_{ij})$ . In this case, low-rank approximation is possible using the eigenvalue decomposition. By transposing the upper triangular component of matrix  $J$  with the lower triangular component, we can transform  $J$  into a real symmetric matrix. At this point, the value of the Hamiltonian of the approximate Ising model (3) remains unchanged. Since matrix  $J$  is real symmetric, it is possible to diagonalize it:

$$J = U\Sigma U^\top.$$

Here, the matrix  $U$  is a real orthogonal matrix comprising the eigenvectors of  $J$ , while  $\Sigma$  is a diagonal matrix comprising the eigenvalues  $\lambda_1 \geq \lambda_2 \geq \dots \geq \lambda_N$  as its components.

Here, the eigenvalues of the matrix  $J$  are shifted by the smallest eigenvalue  $\lambda_N$  so that all eigenvalues are non-negative:

$$J' = J - \lambda_N I,$$

where  $I$  is an  $N$ -dimensional unit matrix. It should be noted that the value of the Hamiltonian remains unaltered even when the interaction coefficients present in the expression (3) are replaced with the shifted matrix  $J'$ . Furthermore, the matrix  $J'$  can be diagonalized using the same matrix  $U$  as the matrix  $J$ :

$$J' = U \Sigma' U^\top,$$

Here, the following equation is obtained:

$$\Sigma' = \begin{pmatrix} \lambda'_1 & & & \\ & \ddots & & \\ & & \lambda'_{N-1} & \\ & & & 0 \end{pmatrix},$$

where  $\lambda'_i = \lambda_i - \lambda_N$ . By using the diagonal matrix formed by taking the  $K$  largest eigenvalues

$$\Sigma'_K = \begin{pmatrix} \lambda'_1 & & \\ & \ddots & \\ & & \lambda'_K \end{pmatrix},$$

and  $N \times K$  matrix  $U_K$ , which has the corresponding eigenvectors in its columns, the interaction matrix is approximated as

$$J' \approx U_K \Sigma'_K U_K^\top. \quad (4)$$

We will discuss this approximation accuracy later. Since the diagonal matrix  $\Sigma'_K$  is semi-positive definite, its square root can be defined. Thus, by writing

$$(\mathbf{v}_1, \dots, \mathbf{v}_N) = (\Sigma'_K)^{1/2} U_K^\top,$$

the relation  $\langle \mathbf{v}_i, \mathbf{v}_j \rangle \approx J_{ij}$  is satisfied. Given that the minimal eigenvalue of the interaction matrix,  $J'$  is 0, it follows that any interaction matrix can be exactly expressed in exact form by FM, provided that  $K = N - 1$ .

The approximation accuracy of the low-rank approximation of the expression (4) is evaluated as follows. The Frobenius norm of the difference between the shifted interaction matrix, denoted by  $J'$ , and the approximate interaction matrix is employed as an indicator of approximation accuracy. In this case, the following formula is obtained:

$$\begin{aligned} \delta J'_k &= \|J' - U_k \Sigma'_k U_k^\top\| \\ &= \sqrt{\sum_{i=k+1}^N (\lambda'_i)^2}. \end{aligned} \quad (5)$$

In other words, the smaller the sum of the squares of the eigenvalues that are ignored, the smaller the error due to the low-rank approximation. This indicates that a low-rank approximation with low approximation error is more feasible when the eigenvalue distribution of the interaction matrix is biased towards small values. Furthermore, the FM hyperparameter  $K$  can be determined in a way that ensures the value of Eq. (5) is less than the allowable value.

## 3.2 Random Initialization

In this study, two random initialization methods are introduced: one based on the energy distribution and the other based on the interaction coefficient distribution. These methods are similar to the initialization method based on eigenvalue decomposition presented in Sec. 3.1, with the distinction that this method focuses exclusively on the interaction terms.

### 3.2.1 Random Initialization Based on Energy Distribution

In the initialization method based on energy distribution, the model parameters are initialized so that the interaction energy distribution of the approximate Ising model and that of the FM model are aligned. The mean and variance are used as the quantities that characterize the energy distribution. As the distribution that each component of the input variable  $\mathbf{x}$  follows is unknown, we consider the energy distribution when each component is determined completely randomly. This is equivalent to considering the energy distribution in the high-temperature limit.

First, we calculate the mean and variance of the interaction energy in the high-temperature limit. The interaction energy is given by

$$H_2(\mathbf{x}) = - \sum_{\substack{i,j=1 \\ (i<j)}}^N J_{ij} x_i x_j$$

At sufficiently high temperatures, the input variables take on the values  $+1$  and  $-1$  independently and with equal probability:

$$\mathbb{E}_{\mathbf{x}}[x_i] = 0, \quad \mathbb{E}_{\mathbf{x}}[x_i^2] = 1 \quad \text{for all } i.$$

Here,  $\mathbb{E}_{\mathbf{x}}$  represents the average of the distribution of the input variable  $\mathbf{x}$ . First, the average of  $H_2(\mathbf{x})$  is given by

$$\mathbb{E}_{\mathbf{x}}[H_2(\mathbf{x})] = - \sum_{\substack{i,j=1 \\ (i<j)}}^N J_{ij} \mathbb{E}_{\mathbf{x}}[x_i] \mathbb{E}_{\mathbf{x}}[x_j] = 0.$$



The equality in the above equation holds regardless of the specific value of  $J_{ij}$ . Next, the variance of  $H_2$  can be written as follows:

$$\begin{aligned}\text{Var}_{\mathbf{x}}[H_2(\mathbf{x})] &= \sum_{\substack{i,j=1 \\ (i<j)}}^N \sum_{\substack{l,m=1 \\ (l<m)}}^N J_{ij}J_{lm} \mathbb{E}_{\mathbf{x}}[x_i x_j x_l x_m] \\ &= \sum_{\substack{i,j=1 \\ (i<j)}}^N J_{ij}^2.\end{aligned}\tag{6}$$

Here, we used the fact that input variables with different indices follow independent probability distributions. Since the variance of the expression (6) differs for each instance, we use the instance average as a feature for the variance of the interaction energy:

$$\mathbb{E}_{\mathbf{J}}[\text{Var}_{\mathbf{x}}[H_2(\mathbf{x})]] = \frac{N(N-1)}{2} \mathbb{E}_{\mathbf{J}}[J_{ij}^2],\tag{7}$$

where  $\mathbb{E}_{\mathbf{J}}$  refers to the average of the distribution of interaction coefficients.

Next, we calculate the mean and variance of the interaction energy of positive FM and negative FM at high temperatures. The interaction energy is given by

$$\hat{f}_{2,\pm}(\mathbf{x}) = \pm \sum_{\substack{i,j=1 \\ (i<j)}}^N \langle \mathbf{v}_i, \mathbf{v}_j \rangle x_i x_j,\tag{8}$$

Here, we consider the case where the model parameters of the interaction coefficients of FM,  $\mathbf{v}_i = (v_{i1}, \dots, v_{iK})$ , ( $i = 1, \dots, N$ ), follow the following independent Gaussian distribution for each component  $v_{ik}$ :

$$v_{ik} \stackrel{\text{iid}}{\sim} \mathcal{N}(0, \sigma_v^2).\tag{9}$$

The average value of the input variable in Eq. (8) is 0, as in the case of the approximate Ising model. The variance of Eq. (8) can be written as follows:

$$\begin{aligned}\text{Var}_{\mathbf{x}}[\hat{f}_{2,\pm}(\mathbf{x})] &= \sum_{\substack{i,j=1 \\ (i<j)}}^N \sum_{\substack{l,m=1 \\ (l<m)}}^N \sum_{k,k'=1}^K v_{ik} v_{jk} v_{lk'} v_{mk'} \mathbb{E}_{\mathbf{x}}[x_i x_j x_l x_m] \\ &= \sum_{\substack{i,j=1 \\ (i<j)}}^N \sum_{k,k'=1}^K v_{ik} v_{jk} v_{ik'} v_{jk'}.\end{aligned}$$

Since this variance depends on the model parameters, we use the mean value of the

model parameter distribution (9) as a feature:

$$\begin{aligned}\mathbb{E}_{\mathbf{v}} \left[ \text{Var}_{\mathbf{x}}[\hat{f}_{2,\pm}(\mathbf{x})] \right] &= \sum_{\substack{i,j=1 \\ (i<j)}}^N \sum_{k=1}^K \mathbb{E}_{\mathbf{v}}[v_{ik}^2] \mathbb{E}_{\mathbf{v}}[v_{jk}^2] \\ &= \frac{N(N-1)}{2} K \sigma_v^4.\end{aligned}\tag{10}$$

Here, we used the independence of the random variable  $v_{ik}$ .

We derive the conditions for the interaction energy distribution of the approximate Ising model to approach that of the FM model. First, the mean values of the distributions are both 0, so they are the same. Next, in order for the variances of the distributions to approach each other, it is sufficient for the following two equations (7) and (10) to be equal. From the above, we can see that in order to initialize an FM with an energy distribution close to that of the approximate Ising model, it is sufficient to generate the model parameters for the FM interaction coefficients from the following probability distribution:

$$v_{ik} \stackrel{\text{iid}}{\sim} \mathcal{N} \left( 0, \sqrt{\frac{\mathbb{E}_{\mathbf{J}}[J_{ij}^2]}{K}} \right).\tag{11}$$

Since the interaction coefficients of the approximate Ising model are given, the average on the right-hand side of Eq. (11) can be replaced with the following sample average:

$$\mathbb{E}_{\mathbf{J}}[J_{ij}^2] = \frac{2}{N(N-1)} \sum_{\substack{i,j=1 \\ (i<j)}}^N J_{ij}^2.$$

### 3.2.2 Random Initialization Based on Coupling Constants Distribution

As will be demonstrated subsequently, if the mean of the distribution of the interaction coefficient, designated as  $J_{ij}$ , is non-negative, the mean and variance of the coefficient distribution of the interaction term in the formula designated as Eq. (3) can be made to align with those of the interaction coefficient distribution of FM with a negative sign. In the event that the mean of the distribution of  $J_{ij}$  is negative, the interaction coefficient distribution of the approximate Ising model can be made to approximate that of FM using a similar procedure by employing positive FM. Accordingly, in the following, we will limit our consideration to the case where the mean of the distribution of  $J_{ij}$  is non-negative.

Let the mean of the interaction coefficient  $J_{ij}$  be  $\mu \geq 0$  and the variance be  $\sigma^2$ . The negative FM model parameter  $v_{ik}$  is an independent random variable that follows the Gaussian distribution below:

$$v_{ik} \stackrel{\text{iid}}{\sim} \mathcal{N}(\mu_v, \sigma_v^2).\tag{12}$$

Here the condition so as to satisfy the following relations is considered:

$$\mathbb{E}_{\mathbf{v}} [\langle \mathbf{v}_i, \mathbf{v}_j \rangle] = \mu, \quad (13)$$

$$\text{Var}_{\mathbf{v}} [\langle \mathbf{v}_i, \mathbf{v}_j \rangle] = \sigma^2, \quad (14)$$

where  $\mathbb{E}_{\mathbf{v}}$  and  $\text{Var}_{\mathbf{v}}$  represent the mean and variance of the distribution in Eq. (12), respectively. First, if we calculate the left-hand side of Eq. (13), we obtain

$$\mathbb{E}_{\mathbf{v}} [\langle \mathbf{v}_i, \mathbf{v}_j \rangle] = K\mu_v^2. \quad (15)$$

Here, Eq. (15) is always nonnegative. Note that, due to this property, it is not possible to match the mean of the distribution of interaction coefficients with negative FM when  $\mu < 0$  with the mean of the approximate Ising model. Next, the left-hand side of Eq. (14) is calculated as

$$\text{Var}_{\mathbf{v}} [\langle \mathbf{v}_i, \mathbf{v}_j \rangle] = K\sigma_v^2 (\sigma_v^2 + 2\mu_v^2) \quad (16)$$

From Eqs. (13)–(16), it is sufficient to generate the model parameters with negative FM from the following probability distribution:

$$v_{ik} \stackrel{\text{iid}}{\sim} \mathcal{N} \left( \sqrt{\frac{\mu}{K}}, \frac{\sqrt{\mu^2 + K\sigma^2} - \mu}{K} \right).$$

Since the interaction coefficients of the approximate Ising model are given,  $\mu$  is replaced with the sample mean and  $\sigma^2$  is replaced with the unbiased variance.

## 4 Approximation Error Analysis with Random Matrix Theory

In this study, we analyze the approximation accuracy of the initialization method for FM based on low-rank approximation, as introduced in Sec. 3.1, using random matrix theory. This analysis demonstrates that as the input dimension increases, the instance dependence of the interaction matrix in the approximation error in Eq. (5) is eliminated. Furthermore, we present a method for determining the effective rank  $K^*$ , which ensures sufficient approximation accuracy.

We begin by considering the case in which the components of the true interaction matrix  $J$  are distributed according to a Gaussian distribution:

$$J_{ij} \stackrel{\text{iid}}{\sim} \mathcal{N}(\mu, \sigma^2), \quad (17)$$

where  $i \leq j$ , the mean of the interaction coefficient is denoted by  $\mu$ , the variance by  $\sigma^2$ , and the input dimension is  $N$ . In the case of a matrix with components that follow a Gaussian distribution with mean zero, the effective rank,  $K^*$ , can be readily derived, as the eigenvalue distribution can be obtained analytically using the random matrix theory. Nevertheless, this is not a straightforward process when dealing with finite means. In this section, we will combine Wigner’s semicircle law [37–39] and the theory of the maximum

eigenvalue distribution theory [40, 41] is employed to derive the effective rank of the interaction matrix  $J$  in Eq. (17).

If we expand  $J$  around the random matrix  $\bar{J}$ , where each component follows a Gaussian distribution with mean 0 and variance  $\sigma^2$ , we obtain:

$$\begin{aligned} J &= \mu \mathbf{1}\mathbf{1}^\top + \bar{J} \\ &= U_\mu \left( \Sigma_\mu + U_\mu^\top \bar{J} U_\mu \right) U_\mu^\top \\ &\stackrel{d}{=} U_\mu \left( \Sigma_\mu + \bar{J} \right) U_\mu^\top. \end{aligned} \quad (18)$$

Since  $\mu \mathbf{1}\mathbf{1}^\top$  is a real symmetric matrix, it can be diagonalized into  $\Sigma_\mu$  using an appropriate real unitary matrix  $U_\mu$ . Additionally, we have used the observation that the probability distribution of the  $\bar{J}$  is invariant with respect to the rotation transformation. The symbol  $\stackrel{d}{=}$  means, as  $N \rightarrow \infty$ , the distribution of the components of the matrices on the left-hand and right-hand sides converges to the identical one. The eigenvectors that comprise the matrix  $U_\mu$  are represented by  $\mathbf{u}_i$ . It is a straightforward to diagonalize  $\mu \mathbf{1}\mathbf{1}^\top$ : the diagonal matrix  $\Sigma_\mu$  has a diagonal component of  $N\mu$ , and the remaining diagonal components are 0. Hence, as the variance of the interaction,  $\sigma^2$ , approaches zero, the rank decreases to one, and as the variance increases, it approaches full rank. In Eq. (18), if we expand the matrix in Eq. (18) in perturbation theory assuming that  $\sigma$  is sufficiently smaller than  $\sqrt{N}\mu$ , the eigenvalues can be approximated as

$$\begin{aligned} \lambda_i &\approx \lambda_i^{(0)} + \mathbf{u}_i^\top \bar{J} \mathbf{u}_i \\ &= \lambda_i^{(0)} + \mathbf{u}'_i{}^\top \bar{\Sigma} \mathbf{u}'_i. \end{aligned} \quad (19)$$

Here, the non-perturbative eigenvalues are represented by  $\lambda_i^{(0)}$  ( $i = 1, 2, \dots, N$ ). A matrix  $\bar{\Sigma}$  is the diagonalization matrix of  $\bar{J}$ , and a new basis,  $\mathbf{u}'_i$ , was used for the diagonalization. In the following analysis, it is assumed that the eigenvalues are arranged in descending order. As the eigenvalues below or equal to the second eigenvalue  $\lambda_2$  are given by  $\lambda_i \approx \mathbf{u}'_i{}^\top \bar{\Sigma} \mathbf{u}'_i$ , it can be seen that the cumulative distribution of eigenvalues can be approximated using that of a random matrix with mean 0. According to Wigner's semicircular law, the maximum and minimum eigenvalues of  $\bar{J}$  approach  $2\sqrt{N}\sigma$  and  $-2\sqrt{N}\sigma$ , respectively, in the limit of  $N \rightarrow \infty$ . If the problem size  $N$  is sufficiently large, the maximum eigenvalue and second eigenvalues of  $\bar{J}$  will converge asymptotically to the same value. Furthermore, it is established that the maximum eigenvalue,  $\lambda_1$ , of the interaction matrix  $J$  with a finite mean,  $N\mu + \sigma^2/\mu$ , approaches  $N\mu + \sigma^2/\mu$  in the limit  $N \rightarrow \infty$  [40, 41]. It thus follows that the maximum eigenvalue  $\lambda_1$ , the second eigenvalue  $\lambda_2$ , and the minimum eigenvalue  $\lambda_N$  of the interaction matrix  $J$  satisfy the following:

$$\begin{aligned} \mathbb{E}[\lambda_1] &\approx N\mu + \sigma^2/\mu, \\ \mathbb{E}[\lambda_2] &\approx 2\sqrt{N}\sigma, \\ \mathbb{E}[\lambda_N] &\approx -2\sqrt{N}\sigma. \end{aligned} \quad (20)$$

Next, the cumulative distribution of the eigenvalues that do not fall within the aforementioned three will be calculated. The cumulative distribution of the eigenvalues of the random matrix with mean 0,  $J$ , follows the Wigner semi-circle law [38] as follows:

$$P_0(\lambda < x) = \int_{-2\sqrt{N}\sigma}^x \sqrt{4N\sigma^2 - t^2} dt. \quad (21)$$

Based on the analysis presented in the formula (19), it can be posited that the eigenvalues of the interaction matrix  $J$  also follow the semi-circle law well, except for the largest eigenvalue  $\lambda_1$ . Indeed, Tao *et al.* have provided a proof of the semicircle law for the case of finite averages [39]. The eigenvalues  $\lambda_i$  ( $i = 2, 3, \dots, N$ ) therefore follow Eq. (21) well.

Based on the above analysis, we can find the cumulative distribution of the eigenvalues of the interaction matrix  $J$ . For simplicity, we normalize the eigenvalues as follows:

$$\hat{\lambda} = \frac{\lambda - \lambda_N}{\lambda_1 - \lambda_N}. \quad (22)$$

Consequently, the expected value of the second eigenvalue,  $\hat{\lambda}_2$ , is approximated by the following expression by using Eq. (20):

$$r \equiv \frac{4\sqrt{N}\mu\sigma}{(\sqrt{N}\mu + \sigma)^2}.$$

The remaining eigenvalues,  $\hat{\lambda}_i$  ( $i = 2, 3, \dots, N$ ), obey Wigner's semicircle law in Eq. (21) well. Therefore, by appropriately determining the coefficients so that the function is continuous at  $x = r$ , we obtain the following:

$$P(\hat{\lambda} < x) = \begin{cases} 1 + \frac{x-1}{(1-r)N} & \text{for } x > r, \\ \frac{1}{N} + \frac{4(N-2)}{\pi N r^2} \int_0^x \sqrt{r^2 - (2t-r)^2} dt & \text{for } x \leq r. \end{cases} \quad (23)$$

This is an approximate function for the cumulative distribution of all eigenvalues when  $\sqrt{N}\mu \gg \sigma$ . Equation (23) was derived in the perturbative regime. However, as we will see later, it is also a suitable approximation in the region where  $\sqrt{N}\mu \approx \sigma$ .

In what follows, we will consider the case where the variance of the interactions,  $\sigma$ , is greater than  $\sqrt{N}\mu$ . In this case, the cumulative distribution of eigenvalues can be effectively approximated by the formula in Eq. (21), as the region is close to a random matrix with a mean of 0. Thus, we have

$$P(\hat{\lambda} < x) = \frac{1}{N} + \frac{4(N-1)}{\pi N} \int_0^x \sqrt{1 - (2t-1)^2} dt. \quad (24)$$

From the above analysis, the approximation of the cumulative distribution of the eigenvalues of the interaction matrix in Eq. (17) is given by Eq. (23) for  $\sqrt{N}\mu \geq \sigma$ , and by Eq. (24) for  $\sqrt{N}\mu < \sigma$ . The cumulative distribution of the eigenvalues obtained using these functions is referred to as the approximate cumulative distribution.

We derive the effective rank  $K^*$  for determining the hyperparameters of FM using the approximate cumulative distribution. We will determine the effective rank of the FM by ignoring eigenvalues whose ratio to the largest eigenvalue,  $\hat{\lambda}_1 = 1$ , is less than  $0 < \alpha < 1$ . The number of eigenvalues that are ignored can be estimated as  $N \times P(\hat{\lambda} < \alpha)$  using the Eqs. (23) or (24). In consequence, the effective rank is given as follows:

$$K^*(\alpha) = N \left( 1 - P(\hat{\lambda} < \alpha) \right). \quad (25)$$

Let the  $K^*$  in Eq. (25) be the predicted rank of FM. The predicted rank,  $K^*$ , is obtained by performing the integral as follows. When  $r < 1$ , we have

$$K^*(\alpha) = \begin{cases} \frac{1-\alpha}{1-r} & \text{for } \alpha > r, \\ 1 + \frac{N-2}{\pi} f\left(\frac{\alpha}{r}\right) & \text{for } \alpha \leq r. \end{cases} \quad (26)$$

When  $r = 1$ , the predicted rank is given as

$$K^*(\alpha) = \frac{N-1}{\pi} f(\alpha). \quad (27)$$

Here,  $f(x) = \arccos(2x-1) - 2\sqrt{x(1-x)}(2x-1)$ .

It has been demonstrated that, if it is known that the elements of the true interaction matrix follow a Gaussian distribution, the predicted rank  $K^*$  can be analytically obtained using the equations in either Eq. (26) or Eq. (27). The application of these methods has the potential to significantly reduce the computational complexity of the algorithm in the previous section. As previously stated, when the interaction matrix is known, it is possible to derive the requisite rank to keep the error given by Eq. (5) below an allowable value, using eigenvalue decomposition. However, since the eigenvalue decomposition generally has a computational complexity of  $O(N^3)$ , this calculation becomes difficult as the input dimension increases. On the other hand, if the normality of the interaction matrix can be confirmed using a test such as the Kolmogorov–Smirnov test [42], it is possible to estimate the predicted rank using Eqs. (26) or (27). In particular, if the mean and variance of the interaction matrix are known, the predicted rank  $K^*$  can be estimated with a computational complexity of  $O(1)$ . In this case, the truncated eigenvalue decomposition up to the top  $K^*$  positions [43] provides a reduction in computational cost to  $O(K^*N^2)$ . From the above, this method also has the effect of enhancing the method presented in the previous section. However, the verification of this assertion will be the subject of future research.

## 5 Results

This section presents the results of a numerical experiment that demonstrates the advantage of the low-rank approximation method for initializing FM in reproducing the approximate interaction matrix, as compared to random initialization methods. Furthermore, we demonstrate that the FM initialized by low-rank approximation can accurately

represent the target model for the predicted rank  $K^*$  of the FM, which is estimated using the random matrix theory. In these analyses, the Sherrington–Kirkpatrick (SK) model [44, 45] is employed as the target approximate Ising model. The Hamiltonian of the SK model is given in Eq. (3). The constant term  $c$  and the magnetic field coefficients  $h_i$  ( $i = 1, \dots, N$ ) are equal to zero, and the interaction coefficients  $J_{ij}$  follow a Gaussian distribution:

$$J_{ij} \stackrel{\text{iid}}{\sim} \mathcal{N}\left(\frac{J_0}{N}, \frac{J_1^2}{N}\right). \quad (28)$$

Here,  $J_0 \in \mathbb{R}$  and  $J_1 \in \mathbb{R}$  are parameters that represent the mean and variance, respectively, normalized with respect to the input dimension  $N$ . In this paper, we assume that  $J_0 = 1$ . To assess the precision of the approximation of the interaction matrix, we utilize the error measured by the Frobenius norm of the discrepancy between the approximated interaction matrix,  $J$ , and the interaction matrix,  $G = (G_{ij})$ ,  $G_{ij} = \langle \mathbf{v}_i, \mathbf{v}_j \rangle$ , which is estimated by the FM:

$$\Delta J = \|J - G\|. \quad (29)$$

The diagonal elements of the interaction matrix do not contribute to the Hamiltonian. Consequently the diagonal elements of  $J$  and  $G$  are set to zero. The error defined in Eq. (29) is referred to as the coupling error. It should be noted that the coupling error is distinct from the error resulting from the low-rank approximation, as defined in Eq. (5). The error resulting from the low-rank approximation is the difference between  $J'$ , whose diagonal elements have been shifted by the smallest eigenvalue, and the interaction matrix of FM. On the other hand, the coupling error represents the difference between the interaction matrix  $J$  and the interaction matrix of the FM, with the exclusion of the diagonal components.

## 5.1 Comparison of Initialization Methods

We conducted numerical experiments to evaluate the performance of the FM initialization method. The SK model instances were created by generating the interaction coefficients in accordance with Eq. (28), resulting in the generation of a dataset comprising spin configurations and the corresponding SK model energies. Each data point in the data set is unique. The FM was initialized using two distinct approaches: the low-rank approximation-based initialization and the random initialization, as detailed in Sec. 3. Subsequently, each FM was trained using the aforementioned dataset. Since the mean and variance of the interaction coefficient distribution are given by Eq. (28), the population mean and variance were used instead of the sample mean and unbiased variance for the purpose of random initialization. The optimization algorithm used in the training is AdamW. The learning rate was set to 0.001, and the number of learning epochs was set to 10,000. The coupling error, as defined in Eq. (29), was calculated from the interaction matrix of the FM after training and the interaction matrix of the SK model. This value was then employed as an indicator of approximation accuracy. A total

of 50 datasets were prepared, each comprising unique data points. The coupling error distribution was then obtained by executing calculations for each dataset. In the case of the random initialization methods, the parameters of FM for interaction coefficients also differ after every 50 calculations.

In order to ascertain which of the random initialization methods introduced in Sec. 3.2 would prove most efficient in reducing the coupling error, a series of numerical experiments were conducted. Figure 1 illustrates the rank dependence of the coupling error, as defined in Eq. (29), for the interaction matrix obtained through training the FM initialized by each random initialization method. The input dimension is  $N = 10$ , and the variance parameter of the interaction coefficient of the SK model is  $J_1 = 0.1$ . The results demonstrate that when the size of the dataset is relatively limited in comparison to the total number of data points, the method of initializing negative FM based on the interaction coefficient distribution can result in reduced coupling errors. In order to estimate interaction coefficients using FMQA, it is essential to train the FM with a limited amount of data. Consequently, in FMQA, initialization of the negative FM based on the interaction coefficient distribution is the most effective among the random initialization methods. We confirmed that this behavior is the same even when the input dimension is increased to  $N = 50$ . As the variance parameter is increased to  $J_1 = 10$ , the difference between the two negative FM initialization methods is diminished. Nevertheless, it is confirmed that the initialization based on the interaction coefficient distribution results in coupling errors that are comparable to or smaller than those based on the energy distribution. Although Fig. 2 depicts the results for a single instance of the SK model, similar results have been confirmed to be obtained for other instances. Hence, among the random initialization methods, it was determined that the approach of initializing negative FM based on the interaction coefficient distribution is the most effective.

Subsequently, a numerical experiment was conducted to compare the initialization method for FM using low-rank approximation, as described in Sec. 3.1, with the random initialization method. As a random initialization method, we employed the negative FM initialization method based on the interaction distribution, since the method has been demonstrated to achieve the lowest interaction error within the random initialization methods, as previously described. The results of comparing the coupling errors for these initialization methods, conducted under identical experimental conditions as those employed in the numerical experiment previously described, are presented in Fig. 2. The results demonstrate that initialization methods employing low-rank approximation can achieve reduced coupling errors when trained on relatively modest datasets. The results presented here are for  $N = 10$ , but the superiority of the initialization method using low-rank approximation for  $N = 50$  has also been confirmed. Hence, the initialization method employing low-rank approximation is more effective than the random initialization method in reproducing the true interaction matrix.

In comparison to the random initialization method, the FM initialization method utilizing low-rank approximation becomes increasingly advantageous as the variance  $J_1$  increases. For the random initialization method, we used the negative FM initialization method based on interaction distribution. Figure 3 illustrates the correlation between the coupling error and the value of  $J_1$  for each initialization method. The input dimension



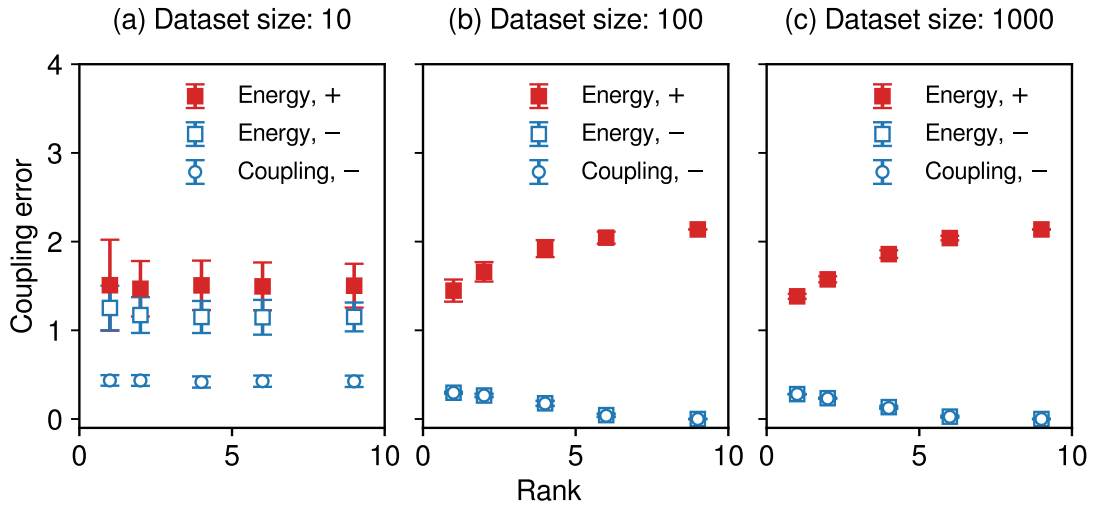


Figure 1: Coupling error by random initialization methods as a function of the rank of FM model. Coupling error for the random initialization method based on energy with positive (negative) FM is represented by red (blue) filled (open) squares, and that for the random initialization method based on coupling with negative FM by blue open circles. Error bar represents standard deviation of the distribution.

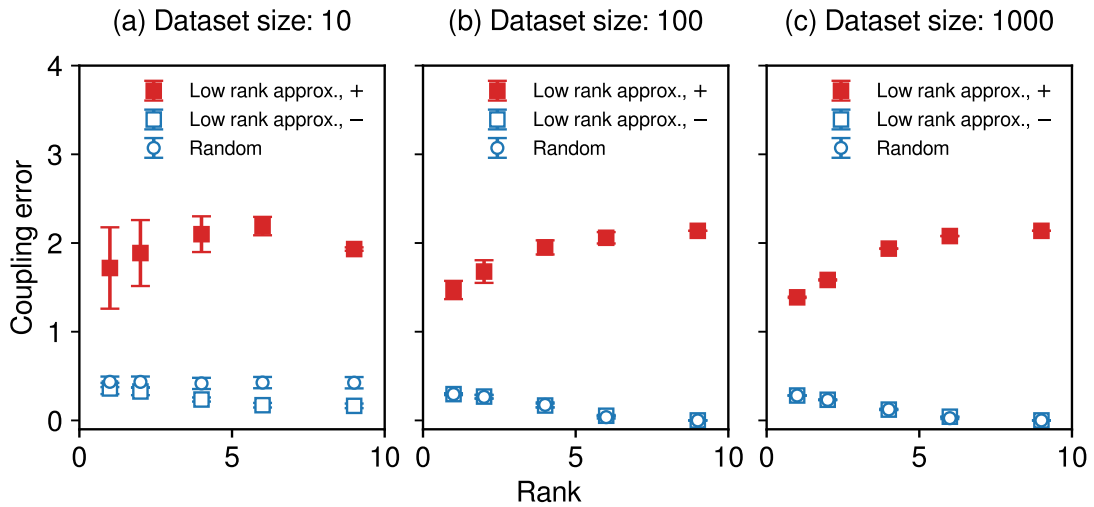


Figure 2: Coupling error for coupling-based random initialization with negative FM and initialization based on eigen decomposition as a function of the rank of FM model. Coupling error for the initialization method based on low rank approximation with positive (negative) FM is shown by red (blue) filled (open) squares, and that for the random initialization method by blue open circles. Error bar represents standard deviation of the distribution.

was  $N = 10$ , the rank of the FM was  $K = 4$ , and the dataset size was 10. The interaction coefficient error increases with  $J_1$ . This is due to the fact that the absolute value of the interaction coefficient increases in direct proportion to  $J_1$ . As the results show, the difference in interaction error between the two initialization methods is amplified as the variance  $J_1$  increases. This behavior was the same even when the input dimension was  $N = 50$ . It can thus be concluded that the initialization method for FM using low-rank approximation is superior even when the value of the variance,  $J_1$ , is altered.

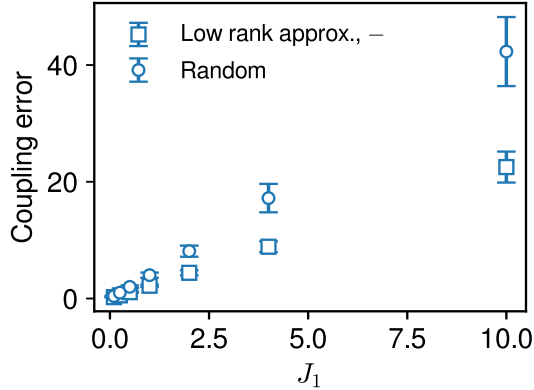
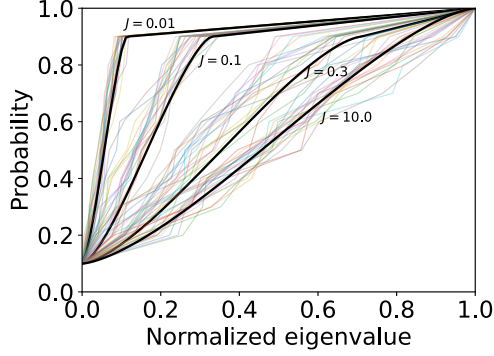


Figure 3: Coupling error for coupling-based random initialization with negative FM and initialization by low rank approximation with negative FM as a function of  $J_1$ . Coupling error for the initialization method based on low rank approximation is represented by blue open squares, and that for the random initialization method by open circles. Error bar represents standard deviation of the distribution.

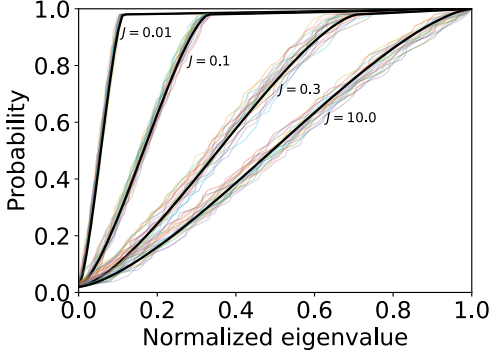
## 5.2 Analysis with Random Matrix Theory

In order to assess the validity of the approximate cumulative distribution derived through the random matrix theory, the following numerical experiments were conducted. Since the interaction coefficients of the SK model are distributed according to a Gaussian distribution, the analysis presented in the Sec. 4 can be applied. In this study, we address the task of estimating the appropriate hyperparameter  $K$  for learning FM using data sampled from the Hamiltonian of the SK model. Here, we fixed  $J_0 = 1$ , generated the interaction matrix using Eq. (17) for  $J_1 = 0.03, 0.1, 0.3, 1.0$  and  $N = 10, 50, 100$ , and generated 20 instances for each combination of these parameters. The eigenvalues were calculated using the eigenvalue decomposition, and the cumulative frequency was plotted after normalization using Eq. (22). The result of the approximate cumulative distribution in addition to the cumulative distribution of the normalized eigenvalues is shown in Fig. 4. The black thick line represents the approximate cumulative distribution based on the random matrix theory. The other solid thin lines represent plots of cumulative distribution of the normalized eigenvalues obtained for each pair of  $(N, J_1)$ .

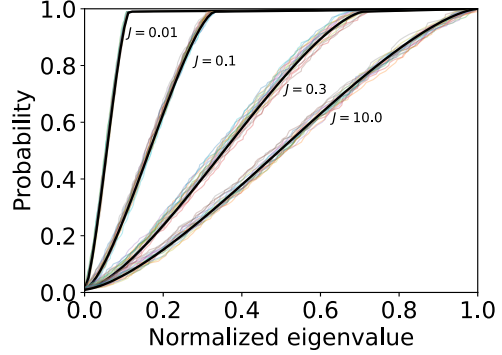
As can be observed, the experimentally determined cumulative distribution aligns with



(a)  $N = 10$ .



(b)  $N = 50$ .



(c)  $N = 100$ .

Figure 4: Numerical and theoretical cumulative probability distributions. The thin solid lines represent numerical cumulative probability distribution. The thick black lines are results obtained by the random matrix theory.

the theoretical lines of the approximate cumulative distribution. Additionally, it was observed that as the input dimension  $N$  increases the agreement between the predicted and actual values improves. This is due to the fact that the variance of the interaction matrix (17) of the SK model converges to zero. For the case  $J_1 > J_0 = 1$ , the results for  $J_1 = 10$  were almost the same as those for  $J_1 = 0.1$ . This is due to the fact that, when the variance is sufficiently large in comparison to the mean, it can be considered to exhibit the behaviour of a random matrix with a mean of zero. In fact, as the value of  $J_1$  increases, the singularity of the second eigenvalue exhibits a positive increase. At  $J_1 = 10$ , the singularity is no longer discernible. The above shows that the approximate cumulative distribution proposed in this study is largely independent of the specific instance details and can accurately describe the cumulative distribution of eigenvalues of

the interaction matrix of the SK model with high accuracy.

We then discuss the results of the error plot of FM with Frobenius norm obtained in the previous section in the context of the random matrix theory. Specifically, we verify that the measured coupling error is sufficiently suppressed at ranks above the predicted rank  $K^*$  given by the Eqs. (26) or (27). Let us consider the case  $J_1 = 0.1$ . Approximation is made to ignore eigenvalues below a fraction  $\alpha = 0.15$  of the normalized maximum eigenvalue. In this case, Eq. (27) produces  $K^* = 5.47$  for  $N = 10$  and  $k^* = 27.82$  for  $N = 50$ . In the case of  $J_1 = 10$ , the rank can be calculated by setting the ratio  $\alpha$  appropriately. In order to achieve an error equal to that of  $J_1 = 0.1$ , you can obviously use the same value as the rank  $K^*$  mentioned above. This is because eigenvalues other than the largest eigenvalue are almost unaffected by the modulation introduced by  $J_1$ , and follow Wigner's semicircle law well. In other words, the value of  $K^*$  is found to be  $K^* = 5.47$  for  $N = 10$  and  $K^* = 27.82$  for  $N = 50$  without determining the ratio  $\alpha$ . Figure 5 shows the error plot of the FM obtained in the previous section together with the above results. Here, the region where the rank is  $K > K^*$  is indicated by the

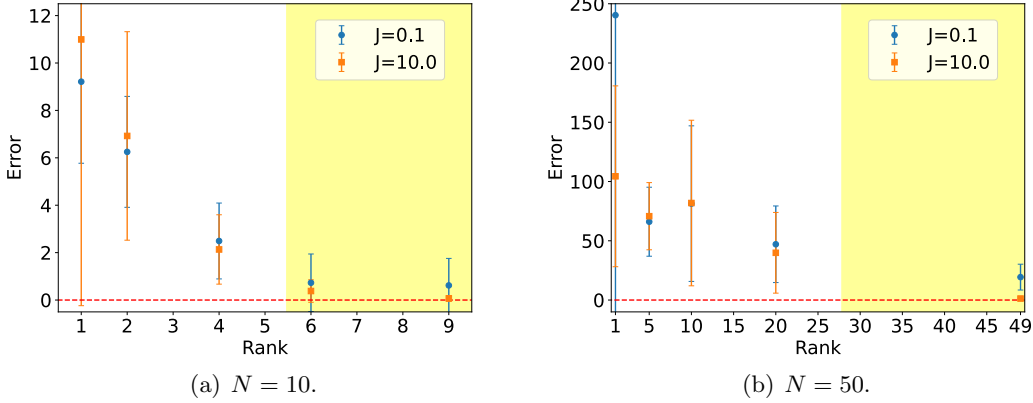


Figure 5: Coupling error and predicted rank. Coupling error obtained by numerical calculations are represented by blue points for  $J_1 = 0.1$  and orange points for  $J_1 = 10$ . The yellow colored region shows that the rank is greater than the effective rank  $K^*$ .

yellow area. The coupling error was normalized by dividing by the variance  $J_1^2$ . From Fig. 5, we can see that for  $N = 10$ , the error is reduced for  $K > K^*$  than for  $K < K^*$  in rank, and the error 0 is reached in the interval of the error bars. Even for  $N = 50$ , when the rank is  $K < K^*$ , the resulting coupling error is large. Conversely, when the rank is  $K = 49$ , which is greater than  $K^*$ , the coupling error is kept close to zero. As described above, the optimal rank of the FM can be determined through the application of the random matrix theory. In the case of a full rank, the interaction matrix can be rigorously decomposed using the FM model. Thus, the ideal scenario would be an error

of 0. However, in the case of  $N = 50$ ,  $J_1 = 0.1$ , a finite error remains. Presumably, this phenomenon is due to the increase in the number of parameters caused by using a large rank, and error did not decrease through the training process. In fact, the literature [22] suggests that a value of  $K$  that is not excessively large should be adopted.

## 6 Conclusion

In this paper, we present a novel initialization method for accurately reproducing an interaction matrix using FM when the interaction matrix is provided approximately. The results of numerical experiments demonstrate that the initialization method based on low-rank approximation is more effective than the random initialization method in obtaining an approximate interaction matrix with greater accuracy. This is achieved by leveraging the statistical properties of the given approximate interaction matrix. Furthermore, the approximation performance of the low-rank initialization method was evaluated using random matrix theory. The findings indicated that as the input dimension augmented, the approximation performance of the low-rank initialization method exhibited diminished dependency on the specific problem instance.

The findings of this study are beneficial for those engaged in optimization using FMQA. One potential application of FMQA is to enhance the approximation accuracy of problems for which the interaction is provided approximately. In this particular application, it is essential to construct an FM that accurately reproduces the approximate interaction matrix. In light of the warm-start method, it is anticipated that a more precise FM model can be constructed by identifying the initial parameters of the FM from the approximate interaction matrix. The findings of this study demonstrate that, when employing the random initialization method, the interaction matrix estimated by the FM gradually diverges from the approximate interaction matrix as the FM training progresses. Conversely, the initialization method for FM based on low-rank approximation allows for the accurate expression of the approximate interaction matrix by FM. It is expected that future research will yield the development of FMQA with high performance based on the findings of this study. In particular, elucidating the performance of FMQA that utilizes the warm-start method represents an intriguing avenue for future investigation.

## Acknowledgement

This work was partially supported by JSPS KAKENHI (Grant Number JP23H05447), the Council for Science, Technology, and Innovation (CSTI) through the Cross-ministerial Strategic Innovation Promotion Program (SIP), “Promoting the application of advanced quantum technology platforms to social issues” (Funding agency: QST), JST (Grant Number JPMJPF2221). This paper is partially based on results obtained from a project, JPNP23003, commissioned by the New Energy and Industrial Technology Development Organization (NEDO). The authors wish to express their gratitude to the World Premier

International Research Center Initiative (WPI), MEXT, Japan, for their support of the Human Biology-Microbiome-Quantum Research Center (Bio2Q).

## References

- [1] Koki Kitai, Jiang Guo, Shenghong Ju, Shu Tanaka, Koji Tsuda, Junichiro Shiomi, and Ryo Tamura. Designing metamaterials with quantum annealing and factorization machines. *Physical Review Research*, 2(1):013319, 2020.
- [2] Tadashi Kadowaki and Hidetoshi Nishimori. Quantum annealing in the transverse Ising model. *Physical Review E*, 58(5):5355, 1998.
- [3] Shu Tanaka, Ryo Tamura, and Bikas K Chakrabarti. *Quantum spin glasses, annealing and computation*. Cambridge University Press, 2017.
- [4] Bikas K Chakrabarti, Hajo Leschke, Purusattam Ray, Tatsuhiko Shirai, and Shu Tanaka. Quantum annealing and computation: challenges and perspectives. *Philosophical Transactions of the Royal Society A*, 381(2241):20210419, 2023.
- [5] Scott Kirkpatrick, C Daniel Gelatt Jr, and Mario P Vecchi. Optimization by simulated annealing. *science*, 220(4598):671–680, 1983.
- [6] David S. Johnson, Cecilia R. Aragon, L. A. McGeoch, and C. Schevon. Optimization by simulated annealing: An experimental evaluation; part i, graph partitioning. *Operations research*, 37(6):865–892, 1989.
- [7] Cecilia R. Aragon, D. S. Johnson, L. A. McGeoch, and C. Schevon. Optimization by simulated annealing: An experimental evaluation; part ii, graph coloring and number partitioning. *Operations research*, 39(3):378–406, 1991.
- [8] M. W. Johnson, M. H. S. Amin, S. Gildert, T. Lanting, F. Hamze, N. Dickson, R. Harris, A. J. Berkley, J. Johansson, P. Bunyk, E. M. Chapple, C. Enderud, J. P. Hilton, K. Karimi, E. Ladizinsky, N. Ladizinsky, T. Oh, I. Perminov, C. Rich, M. C. Thom, E. Tolkacheva, C. J. S. Truncik, S. Uchaikin, J. Wang, B. Wilson, and G. Rose. Quantum annealing with manufactured spins. *Nature*, 473(7346):194–198, 2011.
- [9] R. Barends, A. Shabani, L. Lamata, J. Kelly, A. Mezzacapo, U. Las Heras, R. Babush, A. G. Fowler, B. Campbell, Yu Chen, Z. Chen, B. Chiaro, A. Dunsworth, E. Jeffrey, E. Lucero, A. Megrant, J. Y. Mutus, M. Neeley, C. Neill, P. J. J. O’Malley, C. Quintana, P. Roushan, D. Sank, A. Vainsencher, J. Wenner, T. C. White, E. Solano, H. Neven, and John M. Martinis. Digitized adiabatic quantum computing with a superconducting circuit. *Nature*, 534(7606):222–226, 2016.
- [10] Takahiro Inagaki, Yoshitaka Haribara, Koji Igarashi, Tomohiro Sonobe, Shuhei Tamate, Toshimori Honjo, Alireza Marandi, Peter L McMahan, Takeshi Umeki, Koji

- Enbutsu, et al. A coherent Ising machine for 2000-node optimization problems. *Science*, 354(6312):603–606, 2016.
- [11] D. Rosenberg, D. Kim, R. Das, D. Yost, S. Gustavsson, D. Hover, P. Krantz, A. Melville, L. Racz, G. O. Samach, S. J. Weber, F. Yan, J. Yoder, A. J. Kerman, and W. D. Oliver. 3D integrated superconducting qubits. *npj Quantum inf.*, 3(1):1–5, 2017.
- [12] Masaaki Maezawa, Go Fujii, Mutsuo Hidaka, Kentaro Imafuku, Katsuya Kikuchi, Hanpei Koike, Kazumasa Makise, Shuichi Nagasawa, Hiroshi Nakagawa, Masahiro Ukibe, and Shiro Kawabata. Toward practical-scale quantum annealing machine for prime factoring. *J. Phys. Soc. Jpn.*, 88(6):061012, 2019.
- [13] Sergey Novikov, Robert Hinkey, Steven Disseler, James I Basham, Tameem Albash, Andrew Risinger, David Ferguson, Daniel A Lidar, and Kenneth M Zick. Exploring more-coherent quantum annealing. In *2018 IEEE Int. Conf. on Rebooting Comput. (ICRC)*, pages 1–7. IEEE, 2018.
- [14] Hiroto Mukai, Akiyoshi Tomonaga, and Jaw-Shen Tsai. Superconducting quantum annealing architecture with LC resonators. *J. Phys. Soc. Jpn.*, 88(6):061011, 2019.
- [15] Sanroku Tsukamoto, Motomu Takatsu, Satoshi Matsubara, and Hirotaka Tamura. An accelerator architecture for combinatorial optimization problems. *Fujitsu Sci. Tech. J.*, 53(5):8–13, 2017.
- [16] Maliheh Aramon, Gili Rosenberg, Elisabetta Valiante, Toshiyuki Miyazawa, Hirotaka Tamura, and Helmut G. Katzgraber. Physics-inspired optimization for quadratic unconstrained problems using a digital annealer. *Front. Phys.*, 7:48, 2019.
- [17] Masanao Yamaoka, Chihiro Yoshimura, Masato Hayashi, Takuya Okuyama, Hidetaka Aoki, and Hiroyuki Mizuno. A 20k-spin Ising chip to solve combinatorial optimization problems with CMOS annealing. *IEEE J. Solid-State Circuits*, 51(1):303–309, 2016.
- [18] Hayato Goto, Kosuke Tatsumura, and Alexander R Dixon. Combinatorial optimization by simulating adiabatic bifurcations in nonlinear Hamiltonian systems. *Sci. Adv.*, 5(4):eaav2372, 2019.
- [19] Naeimeh Mohseni, Peter L McMahon, and Tim Byrnes. Ising machines as hardware solvers of combinatorial optimization problems. *Nature Reviews Physics*, pages 1–17, 2022.
- [20] Andrew D. King, Jack Raymond, Trevor Lanting, Richard Harris, Alex Zucca, Fabio Altomare, Andrew J. Berkley, Kelly Boothby, Sara Ejtemaee, Colin Enderud, Emile Hoskinson, Shuiyuan Huang, Eric Ladizinsky, Allison J. R. MacDonald, Gaelen Marsden, Reza Molavi, Travis Oh, Gabriel Poulin-Lamarre, Mauricio Reis, Chris Rich, Yuki Sato, Nicholas Tsai, Mark Volkmann, Jed D. Whittaker, Jason Yao,

- Anders W. Sandvik, and Mohammad H. Amin. Quantum critical dynamics in a 5,000-qubit programmable spin glass. *Nature*, 617(7959):61–66, 2023.
- [21] Andrew Lucas. Ising formulations of many NP problems. *Frontiers in physics*, 2:5, 2014.
- [22] Steffen Rendle. Factorization machines. In *2010 IEEE International Conference on Data Mining*, pages 995–1000, 2010.
- [23] Takuya Inoue, Yuya Seki, Shu Tanaka, Nozomu Togawa, Kenji Ishizaki, and Susumu Noda. Towards optimization of photonic-crystal surface-emitting lasers via quantum annealing. *Optics Express*, 30(24):43503–43512, 2022.
- [24] Yuya Seki, Ryo Tamura, and Shu Tanaka. Black-box optimization for integer-variable problems using Ising machines and factorization machines. *arXiv preprint arXiv:2209.01016*, 2022.
- [25] Tadayoshi Matsumori, Masato Taki, and Tadashi Kadowaki. Application of qubo solver using black-box optimization to structural design for resonance avoidance. *Scientific Reports*, 12(1):12143, 2022.
- [26] Qi Gao, Gavin O Jones, Takao Kobayashi, Michihiko Sugawara, Hiroki Yamashita, Hideaki Kawaguchi, Shu Tanaka, and Naoki Yamamoto. Quantum-classical computational molecular design of deuterated high-efficiency OLED emitters. *Intelligent Computing*, 2:0037, 2023.
- [27] Kenji Nawa, Tsuyoshi Suzuki, Keisuke Masuda, Shu Tanaka, and Yoshio Miura. Quantum annealing optimization method for the design of barrier materials in magnetic tunnel junctions. *Physical Review Applied*, 20(2):024044, 2023.
- [28] Andrejs Tucs, Francois Berenger, Akiko Yumoto, Ryo Tamura, Takanori Uzawa, and Koji Tsuda. Quantum annealing designs nonhemolytic antimicrobial peptides in a discrete latent space. *ACS Medicinal Chemistry Letters*, 14(5):577–582, 2023.
- [29] Akihisa Okada, Hiroaki Yoshida, Kiyosumi Kidono, Tadayoshi Matsumori, Takanori Takeno, and Tadashi Kadowaki. Design optimization of noise filter using quantum annealer. *IEEE Access*, 11:44343–44349, 2023.
- [30] Yannick Couzinie, Yuya Seki, Yusuke Nishiya, Hirofumi Nishi, Taichi Kosugi, Shu Tanaka, and Yu-ichiro Matsushita. Machine learning supported annealing for prediction of grand canonical crystal structures. *arXiv preprint arXiv:2408.03556*, 2024.
- [31] Masaharu Hida, Hiroshi Ikeda, Akito Maruo, Masaru Sato, and Takashi Yamazaki. Topology optimization of analog circuit design via global optimization using factorization machines with digital annealer. *Journal of Advanced Mechanical Design, Systems, and Manufacturing*, 18(6):JAMDSM0076–JAMDSM0076, 2024.



- [32] Junsen Xiao, Katsuhiko Endo, Mayu Muramatsu, Reika Nomura, Shuji Moriguchi, and Kenjiro Terada. Application of factorization machine with quantum annealing to hyperparameter optimization and metamodel-based optimization in granular flow simulations. *International Journal for Numerical and Analytical Methods in Geomechanics*, 48(13):3432–3451, 2024.
- [33] Markus Nagel, Rana Ali Amjad, Mart Van Baalen, Christos Louizos, and Tijmen Blankevoort. Up or down? adaptive rounding for post-training quantization. In *International Conference on Machine Learning*, pages 7197–7206. PMLR, 2020.
- [34] Hiroshi Sampei, Koki Saegusa, Kenshin Chishima, Takuma Higo, Shu Tanaka, Yoshihiro Yayama, Makoto Nakamura, Koichi Kimura, and Yasushi Sekine. Quantum annealing boosts prediction of multimolecular adsorption on solid surfaces avoiding combinatorial explosion. *JACS Au*, 3(4):991–996, 2023.
- [35] Sebastian Prillo. An elementary view on factorization machines. In *Proceedings of the Eleventh ACM Conference on Recommender Systems*, page 179–183, New York, NY, USA, 2017.
- [36] Ming Lin, Shuang Qiu, Jieping Ye, Xiaomin Song, Qi Qian, Liang Sun, Shenghuo Zhu, and Rong Jin. Which factorization machine modeling is better: A theoretical answer with optimal guarantee. In *Proceedings of the AAAI Conference on Artificial Intelligence*, volume 33, pages 4312–4319, 2019.
- [37] Eugene P. Wigner. Characteristic vectors of bordered matrices with infinite dimensions. *Annals of Mathematics*, 62(3):548–564, 1955.
- [38] Eugene P. Wigner. On the distribution of the roots of certain symmetric matrices. *Annals of Mathematics*, 67(2):325–327, 1958.
- [39] Terence Tao. Outliers in the spectrum of iid matrices with bounded rank perturbations. *Probability Theory and Related Fields*, 155:231–263, 2013.
- [40] Donald W. Lang. Isolated eigenvalue of a random matrix. *Phys. Rev.*, 135:B1082–B1084, Aug 1964.
- [41] Peter J. Forrester. Rank 1 perturbations in random matrix theory — a review of exact results. *Random Matrices: Theory and Applications*, 12(04):2330001, 2023.
- [42] David J Sheskin. *Handbook of parametric and nonparametric statistical procedures*. Chapman and hall/CRC, 2003.
- [43] Per Christian Hansen. *Rank-deficient and discrete ill-posed problems: numerical aspects of linear inversion*. Society for Industrial and Applied Mathematics, USA, 1999.
- [44] Scott Kirkpatrick and David Sherrington. Infinite-ranged models of spin-glasses. *Physical Review B*, 17(11):4384, 1978.

- [45] Dmitry Panchenko. *The sherrington-kirkpatrick model*. Springer Science & Business Media, 2013.